DOI: 10.1002/ejic.201000791

$[Fe^{III}(bztpen)(OCH_3)](PF_6)_2$: Stable Methoxide–Iron(III) Complex Exhibiting Spin Crossover Behavior in the Solid State

Norma A. Ortega-Villar,[a,b] M. Carmen Muñoz,[c] and José A. Real*[a]

Keywords: Magnetic properties / Iron / O ligands / Pentadentate ligands / Spin crossover

Complex $[Fe^{III}(bztpen)(OCH_3)](PF_6)_2$ (**1**) crystallizes as the major yellow-brown product from spontaneous oxidation of its corresponding iron(II) counterpart in methanol solution. Magnetic measurements and EPR spectra demonstrate that **1** undergoes a poorly cooperative $^6A_1 \leftrightarrow {}^2T_2$ spin conversion in the temperature range 300–50 K, with characteristic thermodynamic parameters ΔH = 6.15 kJ mol^{-1}, ΔS = 39.88 J K^{-1} mol^{-1}, and $T_{1/2}$ = 154 K. The crystal structure of **1** has been investigated at 100 and 293 K.

Introduction

Spin crossover (SCO) compounds have attracted much attention in recent decades as they represent one of the best examples of switchable molecular materials. In complexes with the electronic configuration $3d^n$ ($4 \leq n \leq 7$), the SCO phenomenon occurs when the energy gap between the high-spin (HS) and the low-spin (LS) states is of the order of magnitude of the thermal energy k_BT. In general, SCO compounds can be switched from one state to the other in a reversible, detectable, and controllable way by the action of external stimuli such as temperature, pressure, light, intense magnetic fields, or even an analyte. Iron(II) and iron(III) SCO complexes have been by far the most investigated.[1]

The SCO phenomenon was discovered by Cambi and Szegö in 1931 in a series of tris(*N*,*N*-disubstituted-dithiocarbamato)iron(III) complexes.[2] Since then, a variety of iron(III) complexes undergoing SCO between the HS (S = 5/2) and LS (S = 1/2) states have been reported. Ligands of the Schiff base type provide the most versatile source of iron(III) SCO complexes.[3] Typically, these complexes display a $[FeN_4O_2]$ coordination environment, which may be achieved by the participation of ancillary ligands This coordination environment has also been achieved in a limited series of iron(III) SCO complexes derived from $[Fe(cat)(tpa)]BPh_4$, where cat^{2-} is the catecholate anion and tpa is the polypyridine-type ligand tris(2-pyridylmethyl)-amine.[4] Iron(III) SCO complexes with the $[FeN_6]$ core are essentially porphyrinate-based complexes.[5]

Recently, we have investigated the formation of $[Fe^{II}(bztpen)(X)]^{n+}$ complexes, where bztpen is *N*-benzyl-*N*,*N*′,*N*′-tris(2-methylpyridyl)ethylenediamine (see Scheme 1) and X is an anion or solvent molecule. The stability of the $[Fe^{II}(bztpen)(X)]^{n+}$ complexes towards oxidation follows the expected spectrochemical series of the exogenous ligand X. The least and most stable complexes are achieved when X is I^- and CN^-, respectively, which is consistent with the solid-state structural and magnetic data obtained for the $[Fe^{II}(bztpen)(X)](PF_6)_n$ series. For halide and pseudohalide ligands (X = Cl^-, Br^-, I^-, OCN^-, and SCN^-), the resulting complex is in a paramagnetic HS state, while the complex is in the diamagnetic LS state when X is $[N(CN)_2]^-$, CH_3CN, or CN^-.[6] Apparently, the crossing point between the HS and LS states occurs between X = SCN^- and CH_3CN or $[N(CN)_2]^-$. Indeed, two- and one-step spin crossover (SCO) behaviors were observed in the solid state and in solution, respectively, for the dinuclear species $[\{Fe^{II}(bztpen)_2\}\{\mu\text{-}N(CN)_2\}](PF_6)_3$.[7]

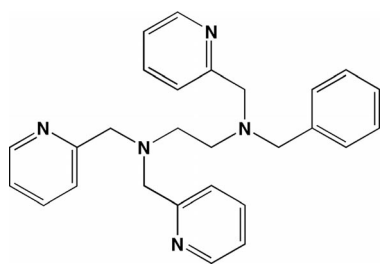

Scheme 1. The ligand bztpen.

[a] Instituto de Ciencia Molecular (ICMol), Universidad de Valencia,
C/ Catedrático José Beltrán Martínez, 2, 46980 Paterna (Valencia), Spain
E-mail: jose.a.real@uv.es
[b] Departamento de Química Inorgánica, Facultad de Química, Universidad Nacional Autónoma de México,
México D.F., 04510, México
[c] Departamento de Física Aplicada, Universidad Politécnica de Valencia,
Camino de Vera s/n, 46022, Valencia, Spain

From these studies, it can be inferred that the polypyridine-like bztpen ligand stabilizes the iron(II) ion reasonably well; however, we have observed that in the absence of coordinating anions the Fe^{II}–bztpen system is unstable in methanol, affording the species $[Fe^{III}(bztpen)(OCH_3)]^{2+}$. Here we report the synthesis and characterization of the iron(III) spin crossover complex $[Fe^{III}(bztpen)(OCH_3)](PF_6)_2$ (**1**). To the best of our knowledge, **1** constitutes the first example of an iron(III) complex comprising a pentadentate polypyridine-type ligand and an exogenous anionic methoxide ligand that undergoes SCO in the solid state.

Results and Discussion

The title compound crystallizes when yellow methanol solutions of the $[Fe^{II}(bztpen)CH_3OH]^{2+}$ species generated in situ are concentrated under a steady stream of argon. The resulting yellow-brown crystals of **1** are made up of the spontaneously oxidized $[Fe^{III}(bztpen)(OCH_3)]^{2+}$ cation, which contains the methoxide anion as exogenous ligand, and two PF_6^- anions (vide infra).

The crystal structure of the title compound was investigated at 100 and 293 K. The molecular structure for **1** in the LS state (T = 100 K) is displayed in Figure 1, together with the atom-numbering scheme. Representative bond lengths and angles are collected in Table 1. Figure 2 shows an overlay of the LS (T = 100 K) and HS (T = 293 K) structures, emphasizing the most important structural modifications upon spin conversion. The crystal remains in the orthorhombic *Pbca* space group at both temperatures. The iron atom is in a distorted octahedral $[FeN_5O]$ environment, whereby the five nitrogen atoms belong to the pentadentate bztpen ligand and the oxygen atom corresponds to the methoxide group, which acts as a monodentate terminal ligand. Two PF_6^- anions balance the charge of the $[Fe^{III}(bztpen)(OCH_3)]^{2+}$ species. The bztpen ligand is wrapped around the iron atom, defining a distorted square pyramid in which the nitrogen atom N(2) lies on the axial apex. This atom is in the center of a tripod whose arms are defined by two picolylamine-like moieties [N(2)–C(7)–C(8)–N(3) and N(2)–C(6)–C(5)–N(1)] and an ethylenediamine-like moiety [N(2)–C(15)–C(14)–N(4)]. These arms are anchored to the iron atom by the atoms N(3), N(1), and N(4), respectively. The average Fe–N bond length is 2.038 and 2.154 Å at 100 and 293 K, respectively. The Fe–O bond length, which is in a *trans* configuration with respect to the N(2) atom, is 1.793(3) Å at 100 K and 1.784(9) Å at 293 K. This short Fe–O bond length is characteristic of iron(III)–methoxide complexes.[8] The variation of the average Fe–N bond length in the $[FeN_5]$ core between the two temperatures is 0.116 Å, whilst the average variation of the complete $[FeN_5O]$ core is 0.096 Å. This value is consistent with the occurrence of a rather complete $^6A_1 \leftrightarrow {}^2T_2$ spin conversion for the iron(III) ion.[9] Typically, this variation is found to be in the range 0.12–0.15 Å for a complete spin conversion. The noticeable increase of the Fe–O bond length upon HS-to-LS conversion is most likely related to the increase of electronic population of the t_{2g} orbitals in the LS state, which enhances electronic repulsion between the t_{2g} orbitals and the π-donating orbitals of the CH_3O^- ligand. The [Fe(bztpen)] moiety is very similar to that described for iron(II)–bztpen complexes.[6,7]

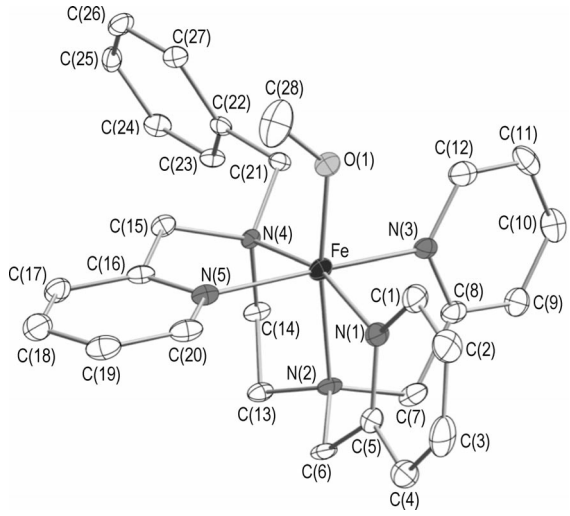

Figure 1. ORTEP representation and atom numbering for **1** in the LS state (T = 100 K). Hydrogen atoms have not been included for the sake of simplicity. Thermal ellipsoids are presented at 50% probability.

Table 1. Selected bond lengths [Å] and angles [°].

	100 K	293 K
Fe–N(1)	2.001(3)	2.095(12)
Fe–N(2)	2.070(3)	2.209(9)
Fe–N(3)	2.000(3)	2.105(11)
Fe–N(4)	2.093(3)	2.224(10)
Fe–N(5)	2.026(3)	2.138(11)
Fe–O	1.793(3)	1.784(9)
N(1)–Fe–N(2)	79.31(13)	75.9(4)
N(1)–Fe–N(3)	94.76(13)	96.0(4)
N(1)–Fe–N(4)	162.66(13)	154.5(4)
N(1)–Fe–N(5)	90.52(14)	90.3(4)
N(1)–Fe–O	99.09(14)	101.8(5)
N(2)–Fe–N(3)	83.02(13)	78.8(4)
N(2)–Fe–N(4)	84.92(12)	80.9(3)
N(2)–Fe–N(5)	92.79(13)	89.6(4)
N(2)–Fe–O	172.02(14)	174.0(4)
N(3)–Fe–N(4)	90.40(12)	89.6(4)
N(3)–Fe–N(5)	172.53(14)	165.1(4)
N(3)–Fe–O	89.35(13)	96.1(5)
N(4)–Fe–N(5)	83.05(15)	79.1(4)
N(4)–Fe–O	97.51(13)	102.3(4)
N(5)–Fe–O	95.05(13)	95.9(4)
Fe–O–C(28)	129.9(3)	153.9(12)

The spin conversion provokes a remarkable change of approximately 24° in the Fe–O–CH_3 bond angle, which increases from 129.9(3)° at 100 K to 153.9(12)° at 293 K. More moderate, but nonetheless remarkable variations [ΔHS-LS] are observed for the angles of the $[FeN_5O]$ core upon spin conversion {Δ[N(1)–Fe–N(4)] = –8.16°, Δ[N(3)–Fe–N(5)] = –7.43°, Δ[N(3)–Fe–O] = +6.75°, Δ[N(4)–Fe–O]

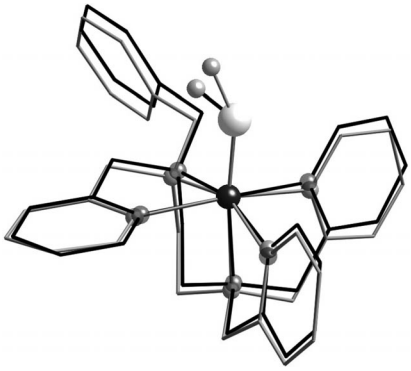

Figure 2. Overlay of the HS (gray) and LS (black) state structures for **1** illustrating the changes upon spin state transition.

= +4.79°, Δ[N(2)–Fe–N(3)] = –4.22°, Δ[N(2)–Fe–N(4)] = –4.02°, Δ[N(4)–Fe–N(5)] = –3.95° and Δ[N(1)–Fe–N(2)] = –3.41°}.

A perspective of the crystal packing along the [100] direction is displayed in Figure 3. This perspective shows an apparent organization of the cationic species by pairs in which the shortest Fe···Fe distances are found to be 9.829(2) Å at 100 K (see molecular units enclosed with dotted line, Figure 3). More precisely, this pair of cations corresponds to the first two members of an infinite zigzag "chain" running along the [100] direction. Within this infinite "chain", there are some C···C contacts shorter than the sum of the van der Waals distance (3.70 Å), namely C(23)···C(11) 3.636(14) Å, C(26)···C(2) 3.602(14) Å, C(24)···C(10) 3.600(14) Å, and C(24)···C(11) 3.584(14) Å. There are no remarkable discrete or extended contacts between the cationic units in other directions of the crystal. In fact, the two crystallographically independent PF_6^- anions act as separators that fill the space between the cations. Furthermore, there are no remarkable contacts between the PF_6^- anions and the cationic units. Thermal displacements of the PF_6^- anions are reasonably small at 100 K; however, clearly the P(2)F_6^- anion is more disordered than the P(1)F_6^- anion at this temperature. At 293 K, the thermal disorder of P(2)F_6^- increases considerably with respect to that of P(1)F_6^-, and this is most likely the cause of the lower accuracy obtained for the structure at 293 K. Nevertheless, the metal-to-ligand bond lengths and angles for **1** compare quite well with those reported for related iron(III) spin crossover compounds.

Figure 4 shows the thermal dependence of the $\chi_M T$ product, where χ_M is the molar magnetic susceptibility and T is temperature. At 310 K, $\chi_M T$ is equal to 4.15 $cm^3 K mol^{-1}$, a value slightly smaller than that expected for iron(III) in the HS state (4.375 $cm^3 K mol^{-1}$, $g = 2$) and clearly higher than that expected for iron(II) in the HS state. The value of $\chi_M T$ decreases continuously as the temperature is lowered to attain a value of approximately 1.35 $cm^3 K mol^{-1}$ in the region 50–10 K. This behavior corresponds to a poorly cooperative spin transition with a certain percentage of HS molecules trapped in the LS state. This poor cooperativeness is consistent with the lack of relevant intermolecular interactions.

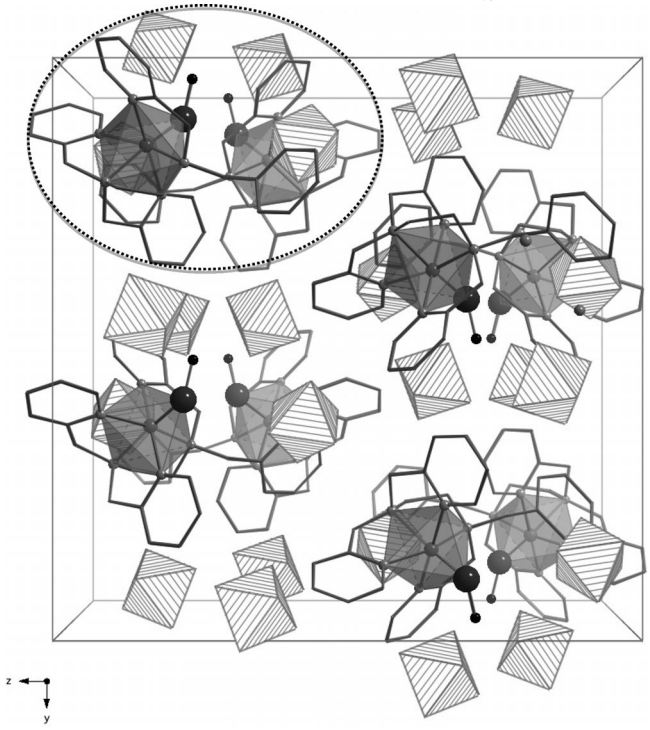

Figure 3. Crystal packing of compound **1** seen along the [100] direction. The dotted line encloses a pair of cationic units displaying the shortest Fe···Fe distance (see text).

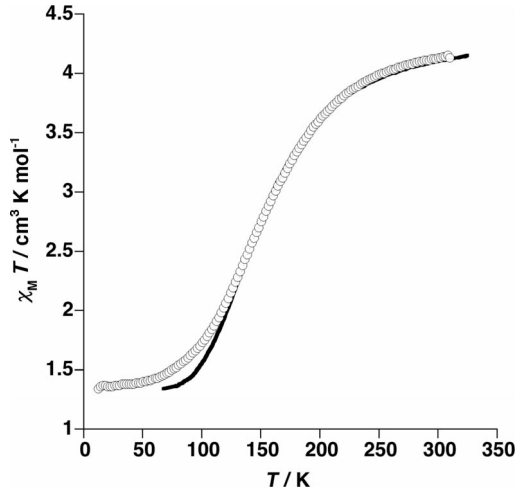

Figure 4. $\chi_M T$ vs. T plot of **1**. The solid line represents the best simulation of experimental data (see text).

The enthalpy, ΔH, and entropy, ΔS, associated with the spin crossover process have been estimated by applying the regular solutions model:[10]

$$\ln[(1 - \gamma_{HS})/(\gamma_{HS} - f_{HS})] = \Delta H/RT - \Delta S/R$$

where $f_{HS} = (\chi_M T)_{LT}/(\chi_M T)_{HS}$ is the residual HS molar fraction, $(\chi_M T)_{LT}$ is the $\chi_M T$ value at low temperature ($T \leq 50$ K), and γ_{HS} is the HS molar fraction expressed as follows:

$$\gamma_{HS} = [(\chi_M T)_m - (\chi_M T)_{LS}]/[(\chi_M T)_{HS} - (\chi_M T)_{LS}]$$

where $(\chi_M T)_m$ is the experimental $\chi_M T$ value, and $(\chi_M T)_{LS}$ and $(\chi_M T)_{HS}$ correspond to the expected values for the fully populated LS and HS states, respectively. The parameters $(\chi_M T)_{LS}$ and $(\chi_M T)_{HS}$ were fixed at 0.5 $cm^3 K mol^{-1}$ (g = 2.3) and 4.4 $cm^3 K mol^{-1}$ (g = 2.0), respectively. ΔH, ΔS, and $(\chi_M T)_{LT}$ have been obtained as adjustable parameters.

The best simulation of the experimental data gives ΔH = 6.15 $kJ mol^{-1}$, ΔS = 39.88 $J K^{-1} mol^{-1}$, and $(\chi_M T)_{LT}$ = 1.44 $cm^3 K mol^{-1}$. The characteristic temperature of the transition $T_{1/2} = \Delta H/\Delta S$ is 154 K. These thermodynamic parameters are quite reasonable as compared with those previously reported for iron(III) spin crossover complexes.[11] The value of ΔS is greater than the electronic spin change expected for a iron(III) ion, $\Delta S_{spin} = R\ln[(2S + 1)_{HS}/(2S + 1)_{LS}]$ = 10.28 $J K^{-1} mol^{-1}$. The remaining entropy variation, approximately 29.6 $J K^{-1} mol^{-1}$, is mainly attributed to intramolecular vibrational changes. The obtained $(\chi_M T)_{LT}$ value indicates that approximately 24% of the molecules remain in the HS state below 50 K. The relatively marked difference between the calculated and observed data for temperatures below 115 K may be due to the presence of sample inhomogeneity.

The EPR spectra of **1** in the temperature range 300–50 K clearly show the $S = 5/2 \leftrightarrow S = 1/2$ spin-state transformation (Figure 5). At 300 K the only significant feature is observed at $g \approx 4.17$ and corresponds to iron(III) in the HS state. As the temperature decreases, a new feature appears around $g \approx 2$, which is characteristic of iron(III) in the LS state. The latter increases in intensity as the temperature decreases down to 50 K. The signal at approximately g = 4.17 persists at lower temperatures, which is in accordance with the magnetic behavior of **1**, in which there is a residual fraction of Fe^{III} ions in the HS state. These EPR spectra are consistent with those previously reported for other iron(III) complexes exhibiting a mixture of HS and LS states.[8b,12]

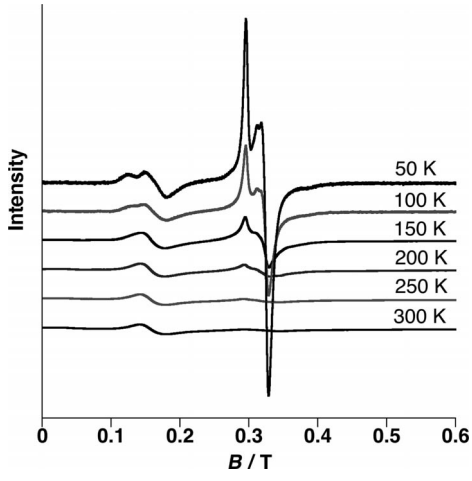

Figure 5. EPR spectra of **1** in the temperature range 300–50 K.

Compound **1** is closely related to complex $[Fe^{III}(PY5)(OCH_3)]^{2+}$ {PY5 = 2,6-bis[bis(2-pyridyl)methoxymethyl]-pyridine}. The latter complex was synthesized by Stack et al. as a biomimetic model for investigating the rate-determining step in the mechanism of lipoxygenase. It was obtained from careful oxidation of the precursor $[Fe^{II}(PY5)(CH_3OH)]^{2+}$ with 0.5 equiv. of H_2O_2. This behavior contrasts with that of the iron(II) precursor of **1**, which oxidizes spontaneously even in an argon atmosphere. This comparative ease of oxidation must be related to the presence of the two amine nitrogen atoms, which confer a more basic character to bztpen with respect to PY5, thereby stabilizing the iron(III) oxidation state under the aforementioned experimental conditions. Although Stack et al. did not check the thermal dependence of the magnetic properties of the ferric species in the solid state, they did observe a thermal variation of the magnetic moment of both compounds in methanol solution from ^1H NMR spectroscopic measurements, suggesting the occurrence of a spin-state conversion in both iron(II) and iron(III) compounds.[8a,8b]

Conclusions

We have demonstrated that, in the absence of coordinating exogenous halide or pseudohalide ligands, methanol solutions of iron(II)–bztpen afford the $[Fe^{III}(bztpen)(OCH_3)]^{2+}$ cation, which is isolated as the PF_6^- salt. Variable-temperature magnetic measurements, EPR spectroscopy, and single-crystal X-ray diffraction analysis demonstrate the occurrence of a spin conversion in the temperature range 50–350 K.

Experimental Section

General Remarks: All manipulations were performed under an argon atmosphere using standard Schlenk techniques. Commercially available reagents and solvents (analytical grade) were used without prior purification.

$[Fe^{III}(bztpen)(OCH_3)](PF_6)_2$ (1): Precursor complex $[Fe^{II}(bztpen)(CH_3OH)]^{2+}$ was prepared in situ by the dropwise addition of a methanol solution of $Fe(BF_4)_2 \cdot 6H_2O$ (5 mL, 0.08 g, 0.24 mmol) to a methanol solution of bztpen (10 mL, 0.10 g, 0.24 mmol) under constant stirring. A further aliquot of methanol (40 mL) was added to the resulting yellow solution before a methanol solution of NH_4PF_6 (ca. 20 mL, 0.12 g, 0.71 mmol) was added. The resulting solution was slowly concentrated under argon for 3–4 days, over which time yellow-brown rectangular crystals of **1** were formed. Yield: 0.082 g, 43%. Green-brown crystals. $C_{28}H_{32}F_{12}FeN_5OP_2$ (800.36): calcd. C 42.02, N 8.75, H 4.03; found C 41.67, N 8.60, H 3.83.

Magnetic Measurements: Variable-temperature magnetic susceptibility measurements were carried out on samples of small crystals of **1** (15–20 mg) by using a Quantum Design MPMS2 SQUID susceptometer equipped with a 5.5 T magnet and operating at 1 T and 1.8–400 K. The susceptometer was calibrated with $(NH_4)_2Mn(SO_4)_2 \cdot 12H_2O$. Experimental susceptibilities were corrected for diamagnetism of the constituent atoms by the use of Pascal's constants.

X-Band EPR Spectra: Variable-temperature electron paramagnetic spectra were carried out on microcrystalline samples of **1** by using a Bruker ELEXYS E580 operating in the range 4–300 K with X

and Q band sources. Magnetic fields 0–2 T; 9.3 GHz/34 GHz cavity and resonators.

X-Ray Crystallography: Diffraction data on single crystals of **1** were collected at 293 and 100 K with a Nonius Kappa-CCD single-crystal diffractometer by using graphite monochromated Mo-K_α radiation (λ = 0.71073 Å). A multiscan absorption correction was performed. The structures were solved by direct methods with SHELXS-97 and refined by full-matrix least-squares on F^2 with SHELXL-97.[13] All non-hydrogen atoms were refined anisotropically. CCDC-784457 (**1** at 100 K) and -784458 (**1** at 293 K) contain the supplementary crystallographic data for this paper. These data can be obtained free of charge from The Cambridge Crystallographic Data Centre via www.ccdc.cam.ac.uk/data_request/cif.

Acknowledgments

This work was supported by the Spanish Ministerio de Ciencia e Innovación (MICINN) and Fondos Europeos para el Desarrollo Regional (FEDER) funds (CTQ2007-64727) as well as the Generalitat Valenciana (GVACOMP2010-139). N. A. O.-V. thanks the Instituto de Ciencia y Tecnología del DF (ICyTDF) in México for a posdoctoral fellowship. We also thank Prof. Víctor Ugalde-Saldívar (Facultad de Química, UNAM, México) for checking the chemical and electrochemical stability of **1**.

[1] a) E. König, *Struct. Bonding (Berlin)* **1991**, *76*, 51; b) P. Gütlich, A. Hauser, H. Spiering, *Angew. Chem. Int. Ed. Engl.* **1994**, *33*, 2024; c) J. A. Real, A. B. Gaspar, V. Niel, M. C. Muñoz, *Coord. Chem. Rev.* **2003**, *236*, 121; d) P. Gütlich, H. A. Goodwin (Eds.), *Spin Crossover in Transition Metal Compounds*, *Top. Curr. Chem.*, Springer, New York, **2004**, vols. 233, 234, 235; e) A. Bousseksou, G. Molnár, G. Matouzenko, *Eur. J. Inorg. Chem.* **2004**, 4353; f) J. A. Real, A. B. Gaspar, M. C. Muñoz, *Dalton Trans.* **2005**, 2062; g) M. A. Halcrow, *Polyhedron* **2007**, *26*, 3523; h) S. Brooker, J. A. Kitchen, *Dalton Trans.* **2009**, 7331.
[2] L. Cambi, L. Szegö, *Ber. Dtsch. Chem. Ges.* **1931**, *10*, 2591.
[3] See for example the following reviews and references therein: a) P. J. van Koningsbruggen, Y. Maeda, H. Oshio, *Top. Curr. Chem.* **2004**, *233*, 259; b) M. Nihei, T. Shiga, Y. Maeda, H. Oshio, *Coord. Chem. Rev.* **2007**, *251*, 2606.
[4] a) A. J. Simaan, M. L. Boillot, E. Rivière, A. Boussac, J. J. Girerd, *Angew. Chem. Int. Ed.* **2000**, *39*, 196; b) A. J. Simaan, M. L. Boillot, R. Carrasco, J. Cano, J. J. Girerd, T. A. Mattioli, J. Ensling, H. Spiering, P. Gütlich, *Chem. Eur. J.* **2005**, *11*, 1779; c) S. Floquet, A. J. Simaan, E. Rivière, M. Nierlilch, P. Thuéry, J. Ensling, P. Gütlich, J. J. Girerd, M. L. Boillot, *Dalton Trans.* **2005**, 1734.
[5] a) W. R. Scheidt, D. K. Geiger, K. J. Haller, *J. Am. Chem. Soc.* **1982**, *104*, 495; b) W. R. Scheidt, Y. Ja Lee, D. K. Geiger, K. Taylor, K. Hatano, *J. Am. Chem. Soc.* **1982**, *104*, 3367; c) M. K. Ellison, H. Nasri, Y. M. Xia, J. C. Marchon, C. E. Schulz, P. G. Debrunner, W. R. Scheidt, *Inorg. Chem.* **1997**, *36*, 4804.
[6] N. Ortega-Villar, V. Ugalde-Saldívar, M. C. Muñoz, L. A. Ortiz-Frade, J. G. Alvarado-Rodríguez, J. A. Real, R. Moreno-Esparza, *Inorg. Chem.* **2007**, *46*, 7285.
[7] N. Ortega-Villar, A. L. Thompson, M. C. Muñoz, V. Ugalde-Saldívar, A. E. Goeta, R. Moreno-Esparza, J. A. Real, *Chem. Eur. J.* **2005**, *11*, 5721.
[8] a) R. T. Jonas, T. D. P. Stack, *J. Am. Chem. Soc.* **1997**, *119*, 8566; b) C. R. Goldsmith, R. T. Jonas, T. D. P. Stack, *J. Am. Chem. Soc.* **2002**, *124*, 83; c) K. Hatano, T. Uno, *Bull. Chem. Soc. Jpn.* **1990**, *63*, 1825.
[9] E. König, *Prog. Inorg. Chem.* **1987**, *35*, 527.
[10] C. P. Slichter, H. G. Drickamer, *J. Chem. Phys.* **1972**, *56*, 2142.
[11] M. Sorai, Y. Nagano, A. J. Conti, D. N. Hendrickson, *J. Phys. Chem. Solids* **1994**, *55*, 317.
[12] A. J. Conti, R. K. Chadha, K. M. Sena, A. L. Rheingold, D. N. Hendrickson, *Inorg. Chem.* **1993**, *32*, 2670.
[13] G. M. Sheldrick, *SHELX97*, *Program for Crystal Structure Determination*, University of Göttingen, Germany, **1997**.

Received: July 21, 2010
Published Online: November 5, 2010

